IEEE Access
Multidisciplinary | Rapid Review | Open Access Journal

Received September 29, 2021, accepted October 10, 2021, date of publication October 21, 2021, date of current version October 26, 2021.

Digital Object Identifier 10.1109/ACCESS.2021.3121196

Determining Optimal SVC Location for Voltage Stability Using Multi-Criteria Decision Making Based Solution: Analytic Hierarchy Process (AHP) Approach

FARUK AYDIN[1], (Student Member, IEEE), AND BILAL GUMUS[2]
[1]Department of Electrical and Electronics Engineering, Faculty of Technology, Marmara University, 34722 İstanbul, Turkey
[2]Department of Electrical and Electronics Engineering, Faculty of Engineering, Dicle University, 21280 Diyarbakır, Turkey

Corresponding author: Faruk Aydin (faruk.aydin@marmara.edu.tr)

This work was supported by the Scientific and Technological Research Council of Turkey (TÜBİTAK) under Project 121E008.

ABSTRACT Due to latest blackouts in the world, voltage instability and voltage collapse have become the main issues studied in electrical power systems. For this purpose, various Flexible AC Transmission Systems (FACTS) devices have been utilized for many years, increasing voltage stability while at the same time improving system performance, reliability, supply quality and providing environmental benefits. These devices location for enhancing voltage stability is a significant problem for actual power networks. When determining the best location of the controller, an optimal solution should be found to increase the loading margin and also reduce voltage deviation and power losses. In the literature, the weight coefficients of the criteria were chosen equally or approximate values were obtained by trial and error method and Multi-Criteria Decision Making (MCDM) techniques have never been used in finding the optimal location of FACTS devices. This article presents a novel technique for optimal location of Static Var Compensator (SVC) devices in power systems using MCDM. The simulation was conducted on Power System Analysis Toolbox (PSAT) in MATLAB. In the proposed approach, IEEE 14-bus, IEEE 30-bus and IEEE 118-bus test systems were used and the optimal location was found out with Analytic Hierarchy Process (AHP), an MCDM technique. The consistency of the results has been checked and the reliability has been increased, and the results of the application are promising. In addition, the optimal location of the SVC for different contingencies was found, and the effects of the overloaded lines and Phase-Shifting Transformer (PST) on the network were analyzed.

INDEX TERMS Voltage stability, optimal location, FACTS, MCDM, PSAT.

I. INTRODUCTION

Voltage stability has a major place in terms of power systems stability. Voltage instability is mainly caused by sagging in reactive power in the grid. Even though this problem is mainly experienced in an area of critical importance, the instability affects the whole power grid [1].

The Power Electronics Technology has offered the opportunity to develop FACTS devices for stable power system operations. Number of power-electronic controllers have been developed and referred to as FACTS in the last two decades. FACTS controllers are intensely used for voltage control. In addition, they are installed in the electrical grid for the purpose of minimizing losses, controlling load flow, improving of transient stability and harmonic mitigation [2].

Shunt capacitors are generally used for reactive power compensation, but they are also installed to reduce power loss and enhance voltage profile of interconnected grid. SVC, due to its low cost and excellent results on power system improvements, is widely used shunt FACTS controller. The loading margin and power transmission capability can be increased by using shunt capacitor, SVC and STATCOM. Nevertheless, with regard to decreasing losses and enhancing the voltage profile, SVC and STATCOM perform better. On the other

The associate editor coordinating the review of this manuscript and approving it for publication was Zhiyi Li.

hand, SVC and STATCOM are more costly than a basic shunt capacitor.

It is difficult and unnecessary to install shunt controllers on all buses because of financial reasons. The identification of the best placement for compensation devices includes calculating the network's stability conditions. However, owing to nonlinearity of the load flow equations, the problem is highly complicated and extensive research must be undertaken to solve it [3].

Multi-objective approaches have become common in latest years for optimum allocation of FACTS controllers. Learning and intelligent optimization methods are used to calculate FACTS devices' optimal placement and capacity. Generally, heuristic algorithms that give the closest solution in a short time are used instead of the mathematical model that gives the most accurate solution. Fitness function centered on several goals is maximized in these methods. Nevertheless, it is not certain that these methods provide the minimum level of satisfaction for the objectives. Selecting suitable weights to show relative importance of different objectives poses another challenge. In the literature, the weight coefficients of the criteria were chosen equally or approximate values were obtained by trial and error method. In previous studies, MCDM methods have never been used to determine these weights in finding the optimal location of various FACTS devices. In some of these articles, criteria weights were considered equal [4]–[21]. In some other articles, criteria weights determined by the decision maker were used [22]–[31]. In some publications, weights were used both equally and at the values determined by the decision maker and in different combinations according to different scenarios [32]–[36]. In all these studies, decision makers determined criteria weights according to their own importance levels, but did not control their consistency. To put it more clearly, authors determined random weights in the selection process, and did not base this on a scientific basis. Therefore, it is clear that there is a significant deficiency in the reliability of the results. This study mainly aims to fill this gap in the literature.

In view of the above, this article addresses the most suitable placement of SVC as a constrained multi-objective optimization problem. For this purpose, the multi-objective optimization problem is converted into a single objective function using the MCDM technique. In this proposed method, considering the operation and load constraints, three objectives are achieved simultaneously while the SVC controller is in the optimal location: increasing the range to loading margin, reducing the bus voltage deviation and minimizing the power losses. The obtained results have shown the efficiency of the suggested method.

II. FACTS DEVICES

A. FACTS CONTROLLERS

The traditional concepts and practices of energy systems have altered during latest years. Better use of the existing energy systems by installing FACTS devices is essential to boost capacities [28].

The philosophy behind the FACTS devices is to use power electronics to control power flow in a grid, enabling complete loading of the transmission line. Power electronic controlled devices such as SVCs; have been used for many years in electrical power systems. N. Hingorani, however, introduced the FACTS concept as a philosophy of total network control [37], [38].

The FACTS controller devices can be categorized as series controllers, shunt controllers, combined series-shunt controllers and combined series-series controllers. Depending on the compensation level, the series compensator is the best choice to increase the power transfer capacity. The shunt compensator is the best option to increase the stability margin. In fact, for a given operating point, if a transient fault occurs, all compensators considerably increase the stability margin. However, this is mainly true for shunt compensation [38]. Conventional compensation is commonly done with reactive power capacitors connected in parallel to the system. Conventional compensation systems may be sufficient for slow load changes and steady state operation. However, under rapidly changing load conditions, the response time may increase and there may be a delay in providing reactive power. In addition, since the contactors switch without considering the grid voltage and the voltage on the compensator, high transient currents may occur on the capacitors. FACTS devices are used because conventional compensation methods have such disadvantages and cause several power quality problems. This study focused on voltage stability. Therefore, shunt FACTS device-SVC is selected for application. SVC was preferred because it is cheaper than STATCOM and Unified Power Flow Controller (UPFC) in terms of total cost [39]. Also, the literature was reviewed and it was determined that SVC is the most widely used FACTS device due to its low cost and positive effect on system performance [40].

B. MODELLING OF SVC

SVC is most commonly described as a shunt-connected static reactive power generator or absorber, consisting of a capacitor and a thyristor-controlled reactor [41]. Fig. 1-a shows the SVC's main structure for one phase. Fig. 1-b presents equivalent circuit of SVC. In practice, a SVC is regarded a variable reactance with the limited ranges of firing angle. The reactive power and current injected into the bus k are calculated with Eq. (1) and (2).

$$I_{SVC} = jB_{SVC}.V_k \tag{1}$$

$$Q_{SVC} = B_{SVC}.V_k^2 \tag{2}$$

where I_{SVC} and Q_{SVC} are the injected/absorbed reactive current and reactive power of SVC respectively. B_{SVC} is the susceptance of the SVC and V_k is the voltage of the bus at which SVC is connected [42]

III. MULTI-CRITERIA DECISION MAKING

MCDM can be described as problems where multiple criteria are optimized, ranked and the best alternative is chosen.

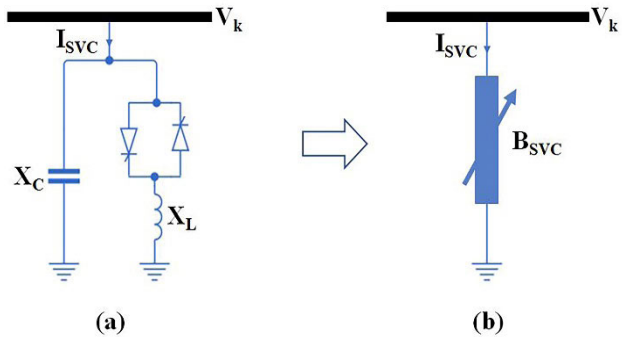

FIGURE 1. The equivalent circuit of SVC.

Nowadays, the difficult and complex decision processes need to be supported by decision making tools that will enable the decision maker to make more efficient, fast and accurate decisions as well as individual skills and experiences.

In the literature there are numerous MCDM methods (e.g. Analytic Hierarchy Process (AHP), Analytic Network Process, MOORA, ELECTRE, VIKOR, PROMETHEE, TOPSIS, ORESTE, ARAS, COPRAS etc.). These methods can be applied to selection, sorting and ranking problems. When choosing the MCDM method to be used, factors such as interdependence of criteria, relations between criteria, computability and simplicity should be taken into account. For example, Analytical Network Process or some fuzzy MCDM methods are used in problems where computation time is important. The aim of this study is to accurately determine the most suitable location and to increase the reliability of the results. AHP is the most preferred method of MCDM as it provides significant convenience to users in terms of computability and comprehensibility. Therefore, in this paper AHP method have been implemented to determine weights of criteria.

A. AHP

AHP is the MCDM method that T. L. Saaty developed in the 1970s. AHP method aims to compare alternatives in pair-wise for criteria and criteria weights, also systematically evaluates several data or elements simultaneously. This technique determines the comparative importance and meaning of each element in the hierarchy. These numerical values represent the weights or priorities [43]. The first stage is the creation of a hierarchical model. In the concepts section, this problem is clarified in more detail. In the second step, pair-wise comparison matrices are constructed. According to expert guidance, matrices are constructed to show the comparative importance of each variable, for all levels in a hierarchical system using values varying from 1 to 9 with ranges of 2 to show equally important, moderately important, strongly important, very strongly important and extremely important, respectively. In the case when five levels are insufficient, 2, 4, 6 and 8 are used as the adjacent medians [44].

After calculating pair-wise comparisons, eigenvalue λ_{max} is used to determine the consistency index *CI*. Decision consistency can then be checked by calculating the consistency ratio *CR* for the appropriate matrix size. If the *CR* value is below 0.1, the decision matrix is acceptable. For other cases, judgement matrix is inconsistent. In these cases, decisions should be revised and enhanced in order to achieve a consistent matrix [45]. As shown in Fig. 2, the AHP technique can be expressed in series of steps [44].

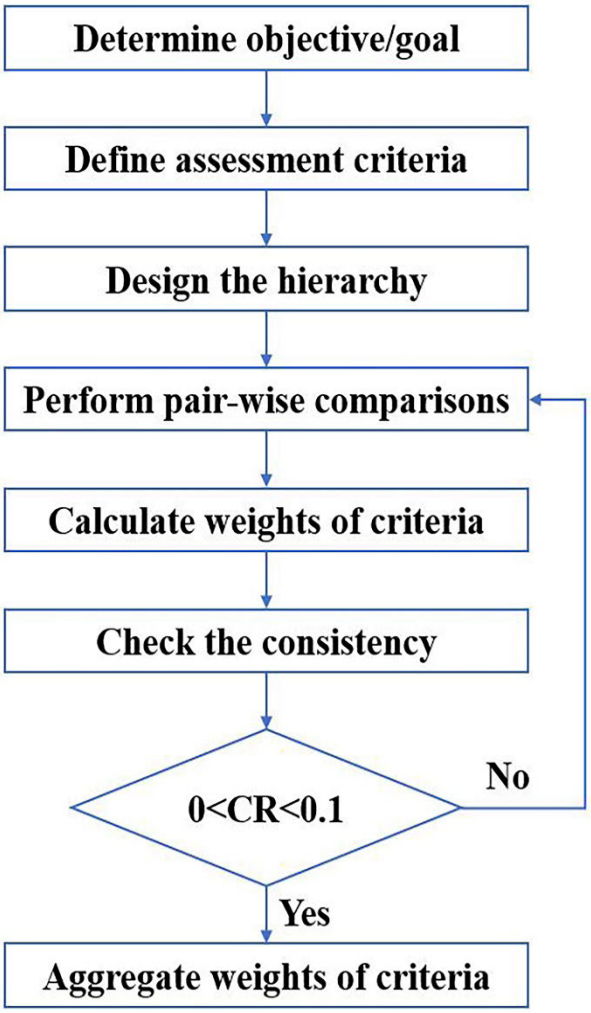

FIGURE 2. Flow chart of the AHP.

B. MULTI-CRITERIA DECISION MAKING CONCEPTS

In decision analysis, each alternative should evaluate according to the pre-defined criteria by the decision maker. In this study, N_A alternatives and N_O criteria show the number of different load buses and the objectives respectively. In the AHP method, hierarchy is formed at least three levels: global goal (first level), individual objectives (second level) and alternatives (third level) [46]. The solution structure of AHP is hierarchically presented in Fig. 3.

After determining the global goal at the first level, objective and pair-comparison matrices should be defined. The N_O objectives found in the second level are either weighed using

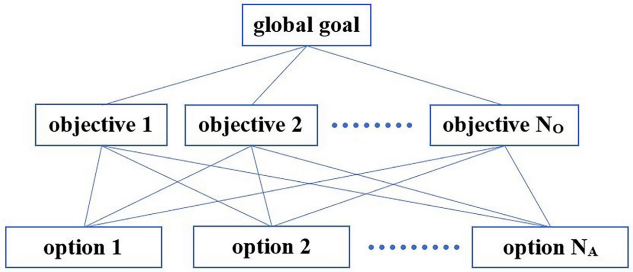

FIGURE 3. AHP structure with three levels.

the same weight (all weights $w^{(j)}$ equal $1/N_O$), or a different definition of weight, as per the preference of the decision maker. Each of the N_A options at the third level are evaluated at the second level with regard to the N_O objectives [46]. B objective matrix, symbolizes the connections between the objectives and alternatives, and b_{ij} is performance value of *ith* alternative with respect to *jth* objective.

$$B = \begin{bmatrix} b_{11} & \dots & b_{1N_0} \\ \vdots & \ddots & \vdots \\ b_{N_A1} & \dots & b_{N_AN_0} \end{bmatrix} \tag{3}$$

At the third level, N_O pair-comparison matrices, symbolized as $D^{(j)}$, are formed. The elements of this matrix show the decision maker's personal preferences. These elements are quantitative assessments made for one objective at once. Quantification is performed with a ratio of nine levels (Table 1) defined in terms of the scale of the Saaty [47]. The $D^{(j)}$ matrix is created with the reciprocal of each element in its symmetrical position. The principal diagonal elements are all equal to 1 [46].

TABLE 1. The Saaty's Scale for comparative judgements used in the AHP methodology.

Entry $d_{pk}^{(j)}$	Description
1	Equally importance
3	Moderately importance
5	Strongly importance
7	Very strongly importance
9	Extremely importance
2, 4, 6, 8	Intermediate levels of importance

In the AHP method, the matrix $D^{(j)}$ must be consistent, meaning the following multiplying condition must be satisfied by the entries in the matrix [48]:

$$d_{kp}^{(j)} = d_{kw}^{(j)}.d_{wp}^{(j)} \tag{4}$$

The comparison between the alternatives, however, cannot allow a perfect verify the consistency with the discrete and amplitude-limited Saaty's scales. To this end, AHP method can be used for values below CR consistency ratio predefined by matrix size and CR value can be determined as follows:

$$CR^{(j)} = CI^{(j)}/RI \tag{5}$$

where

- The consistency index $CI^{(j)}$ is calculated based on the maximum eigenvalue $\lambda_{max}^{(j)}$ as:

$$CI^{(j)} = \frac{\lambda_{max}^{(j)} - N_A}{N_A - 1} \tag{6}$$

- The reference consistency index RI is shown in Table 2, and its value is determined by considering the N_A. The index $CI^{(j)}$ is compared with RI and the matrix $D^{(j)}$ is regarded as consistent if $CI^{(j)} < 0.1$.

TABLE 2. Average random consistency (RI).

Size of matrix	3	4	5	6	7	8	9	10
Random consistency	0.58	0.9	1.12	1.24	1.32	1.41	1.45	1.49

It must be noted that only the scale of Saaty and definition of multiplicative consistency based upon Eq. (4) can confirm the condition in the ratio of $CR^{(j)}$ [46].

IV. PROPOSED METHODOLOGY

A. CONTINUATION POWER FLOW METHOD

In this study, Continuation Power Flow (CPF) was used to determine the system's peak loadability limit. The CPF technique calculates the value called the maximum loadability margin λ_{max}, corresponding to the point of voltage collapse in the nose curve. In power systems, CPF method is widely used for load flow problems. Unlike other power flow techniques, in CPF, the entire nose curve is obtained even after the voltage collapse point (critical point). The CPF method uses the predictor-corrector technique to obtain the PV or λV nose curve, as shown in Fig. 4 [49], [50]. The critical point in the PV curve shows the maximum loadability of the system. At normal initial load conditions, λ can be increased to estimate an approximate solution by a tangent predictor. The correction step for a conventional load flow determines the complete solution [51].

B. OBJECTIVE FUNCTION

Generally, a multi-objective optimization problem requires simultaneously optimized a series of objectives which is linked with equality and inequality constraints [52]. Identified objectives in this article are explained below.

- Loading Margin

The improvement of voltage stability is accomplished with commonly used voltage collapse proximity index, called Voltage Stability Margin (VSM) or Load Margin maximization. This value is the largest load change that can be sustained by the power system at reference operating point in a bus or group of buses. In our problem, the goal is to determine minimum value of the sum of objective functions. Thus, the maximization of VSM can be presented as inverse of maximum loadability:

$$f_1 = 1/\lambda_{critical} \tag{7}$$

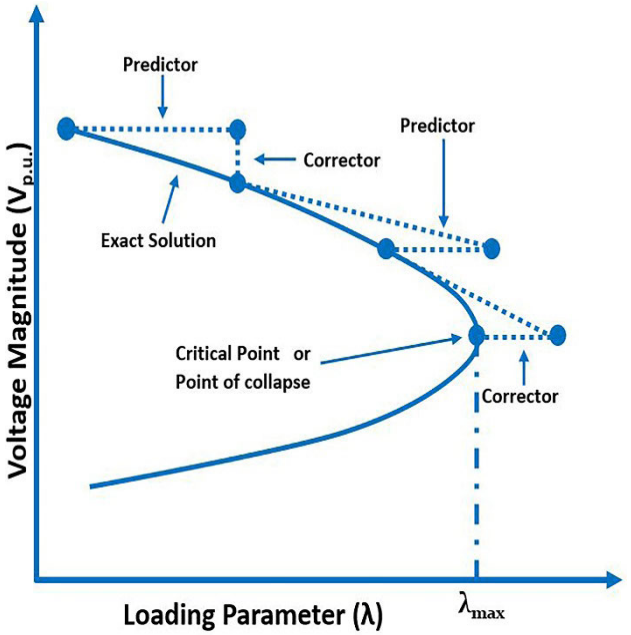

FIGURE 4. Predictor-corrector scheme used in the CPF.

where $\lambda_{critical}$ indicates the loading factor value at the critical point. This value corresponds to the λ_{max} value in the CPF method [53].

- Voltage Deviation

Inacceptable service quality can be caused by overly low voltages, causing voltage instability problems. The FACTS controllers should be connected to optimal placements to improve the voltage profile of the system and to prevent voltage collapse. Therefore, minimizing the bus voltage deviation has been identified as the second aim [54]. This objective function can be calculated as shown in Eq. (8):

$$f_2 = \sum_{m=1}^{N} \left| V_{mref} - V_m \right| \tag{8}$$

where V_m is the voltage magnitude at bus m, V_{mref} is the nominal voltage of bus m and N is the number of buses. In this study, acceptable bus voltage range is selected in the range 0.90 −1.10 p.u.

- Active power losses

From a financial perspective, active power losses (P_{loss}) should also be minimized [53]. P_{loss} can be represented as follows:

$$f_3 = P_{loss} = \sum_{m=1}^{N} g_m \left[V_i^2 + V_j^2 - 2V_iV_j\cos(\delta_i - \delta_j) \right] \tag{9}$$

where, g_m is the conductance of transmission line, V_i is the voltage of bus i, V_j is the voltage of bus j, δ_i is the voltage angle of bus i, δ_j is the voltage angle of bus j.

The objective function can be formulated as shown in Eq. (10) by considering the equality and inequality constraints.

$$\text{Minimize F} = [\text{f}_1, \text{f}_2, \text{f}_3] \tag{10}$$

TABLE 3. Pair-wise comparison matrix of the criteria.

	Loading Margin	Voltage Deviation	Active Power Losses	Priorities
Loading Margin	1	5	7	0.724
Voltage Deviation	1/5	1	3	0.193
Active Power Losses	1/7	1/3	1	0.083

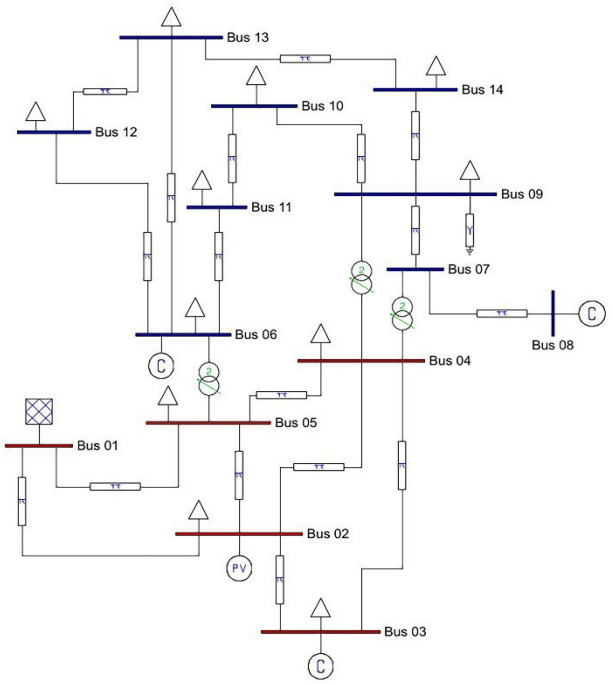

FIGURE 5. IEEE 14-bus system's PSAT model.

The functions f_1, f_2 and f_3 are defined above.

$$F = \omega_1 \text{f}_1 + \omega_2 \text{f}_2 + \omega_3 \text{f}_3 \tag{11}$$

Subject to:

$$\omega_1 + \omega_2 + \omega_3 = 1 \tag{12}$$

$$0 < \omega_1,\ \omega_2,\ \omega_3 < 1 \tag{13}$$

where, ω_1, ω_2 and ω_3 are weighting factors of VSM objective function, voltage deviation objective function and active power losses objective function respectively. While determining the weighting factors of multi-objective optimization, the priorities of the decision maker are taken into consideration. For this reason, voltage stability has been determined as the main problem in the case study presented here. VSM exerts the greatest influence on the voltage stability, while voltage deviation and active power losses have less influence on the voltage stability. The pair-wise comparison matrix showing the criterion importance is given in Table 3. The coefficients (weights) ω_1, ω_2 and ω_3 are calculated by AHP method to 0.724, 0.193 and 0.083 respectively.

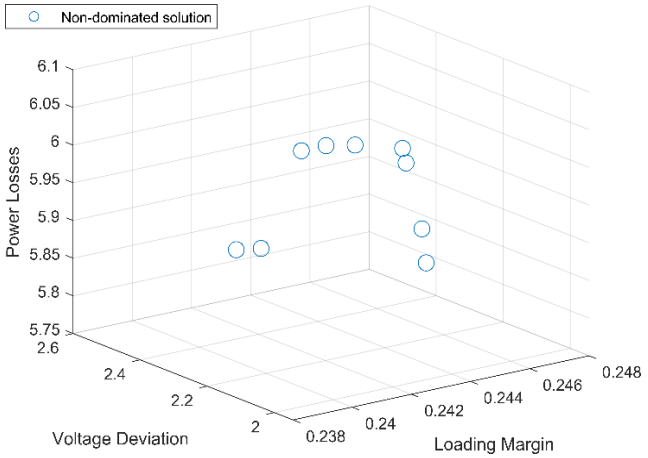

FIGURE 6. Optimal location of SVC for three objectives.

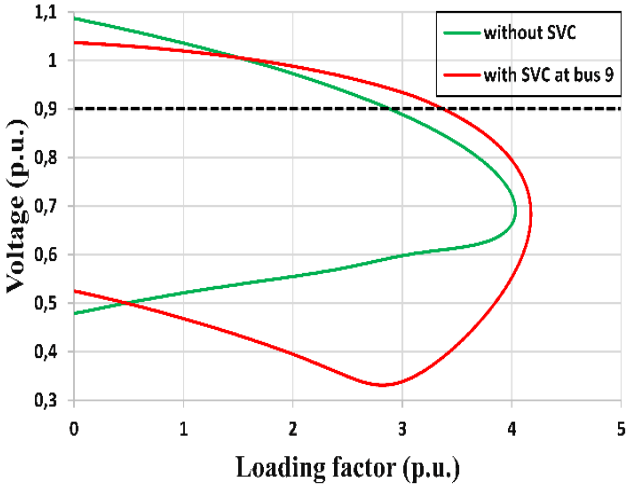

FIGURE 7. PV curves for IEEE 14-bus system without SVC and with SVC at bus 9.

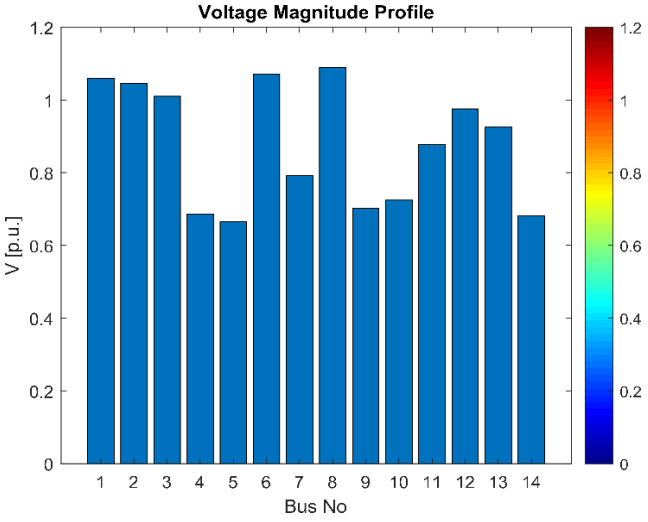

FIGURE 8. IEEE 14-bus system's voltage profile without SVC.

V. SIMULATION RESULTS AND DISCUSSION

In order to improve voltage stability, the simulation method includes determining the optimal bus location for SVC. Optimal SVC location is determined by placing compensator at various buses in test systems and running CPF. To this end, PSAT software in MATLAB is used [55]. In MCDM based programming, the optimal place is determined.

- IEEE 14-bus

The proposed method is tested on IEEE 14-bus system. Fig. 5 shows the IEEE 14-bus network. There are five synchronous machines in this system, generators at bus 1 and 2, and synchronous capacitors for reactive power support at bus 3, 6 and 8. Test system consists of 20 transmission lines and 14 buses with 11 loads. Total active and reactive loads in the system are 259 MW and 77.4 MVAr respectively.

TABLE 4. Minimum values of objective function in IEEE 14-bus test system.

Bus No.	f_1	f_2	f_3	F
4	0.1109	0.1225	0.1091	0.1130
5	0.1108	0.1253	0.1089	0.1135
7	0.1104	0.1110	0.1124	0.1107
9	0.1097	0.1006	0.1135	**0.1082**
10	0.1100	0.0998	0.1134	0.1083
11	0.1117	0.1077	0.1119	0.1109
12	0.1134	0.1212	0.1080	0.1144
13	0.1125	0.1134	0.1096	0.1124
14	0.1106	0.0984	0.1132	0.1085

Bold value shows the most suitable location where the objective function is minimum.

TABLE 5. Optimal location of SVC for different contingencies.

Contingency	From bus	To bus	F	Optimal SVC location
Line 1 Outage	2	5	0.8759	Bus 14
Line 2 Outage	6	12	1.1024	Bus 14
Line 3 Outage	12	13	1.0595	Bus 10
Line 4 Outage	6	13	0.9672	Bus 10
Line 5 Outage	6	11	1.0263	Bus 11
Line 6 Outage	11	10	1.0357	Bus 4
Line 7 Outage	9	10	1.0524	Bus 14
Line 8 Outage	9	14	0.7809	Bus 9
Line 9 Outage	14	13	0.8127	Bus 4
Line 10 Outage	7	9	0.7897	Bus 9
Line 11 Outage	1	2	0.7281	Bus 9
Line 12 Outage	8	7	1.0162	Bus 9
Line 13 Outage	3	2	0.7085	Bus 9
Line 14 Outage	3	4	1.0130	Bus 14
Line 15 Outage	1	5	1.2792	Bus 14
Line 16 Outage	5	4	1.1218	Bus 14
Line 17 Outage	2	4	0.8674	Bus 14
Line 18 Outage	4	9	1.0335	Bus 14
Line 19 Outage	5	6	0.6647	Bus 14
Line 20 Outage	4	7	0.9129	Bus 14

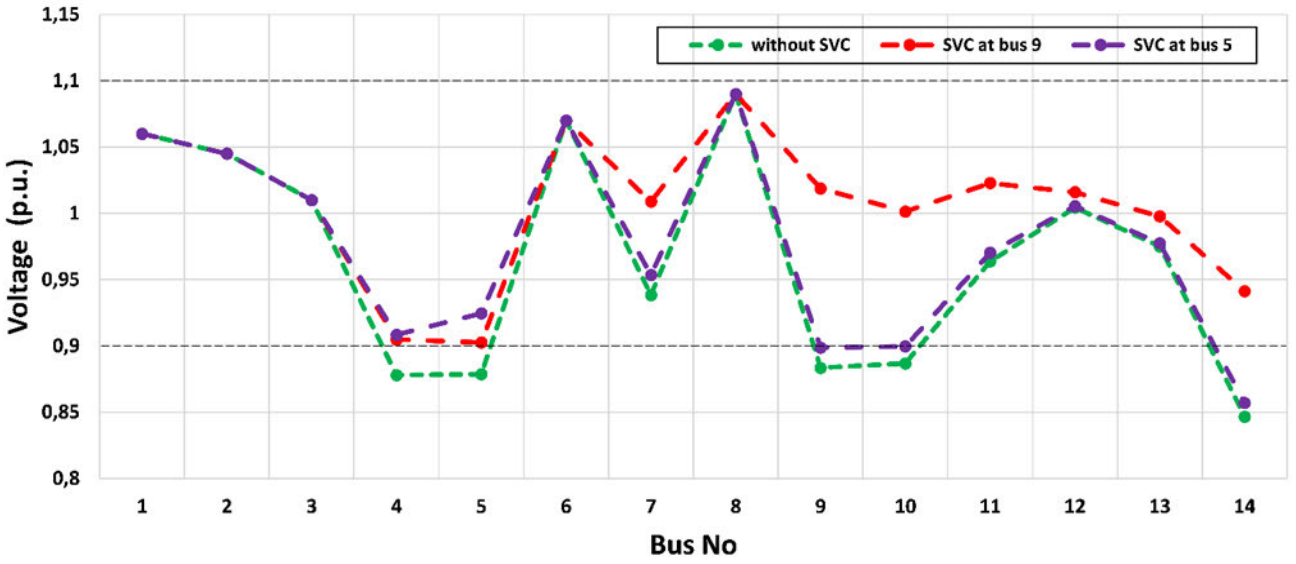

FIGURE 9. Voltage profile of test system without SVC, with SVC at bus 5 and with SVC at bus 9.

TABLE 6. Loading factor, power losses and bus voltage values according to PST angle.

Phase angle		+45°	+30°	+15°	0	-15°	-30°	-45°
Loading factor		3.863	3.956	4.009	4.031	4.018	3.980	3.911
Bus voltages	V_4	0.683	0.667	0.680	0.686	0.685	0.678	0.700
	V_5	0.698	0.668	0.670	0.665	0.652	0.630	0.645
	V_7	0.740	0.748	0.775	0.792	0.800	0.801	0.818
	V_9	0.639	0.651	0.684	0.702	0.709	0.708	0.723
	V_{10}	0.667	0.679	0.708	0.724	0.729	0.728	0.738
	V_{11}	0.846	0.853	0.869	0.876	0.878	0.875	0.878
	V_{12}	0.970	0.971	0.973	0.975	0.976	0.976	0.978
	V_{13}	0.916	0.917	0.922	0.925	0.925	0.924	0.926
	V_{14}	0.627	0.638	0.666	0.681	0.687	0.688	0.699
Power losses		5.582	6.085	6.037	6.015	6.038	6.095	5.589

Since the reactive power limits of the generator are taken into account, the objective function F is calculated at a loading factor near to the critical point. Fig. 6 demonstrates SVC's optimal location for three objectives.

Criteria values in the decision matrix were converted to proportional values in order not to dominate to each other. Table 4 shows the calculation results of the proposed approach and also emphasizes that the best place for SVC is bus 9 in this test system.

Table 4 obviously demonstrates the importance of the MCDM technique used in this study in combining identified objectives and sustaining the minimum level of satisfaction for the objective function. It can be observed from Table 4 that bus 12 provides minimum power losses but, loading margin is not acceptable. Similarly, bus 14 gives the best value in voltage deviation and desirable value in loading margin but, active power loss is very high. The comparison outcomes for loading factor and voltage profile without SVC and with SVC connected at bus 9 are shown in Figs. 7, 8 and 9 respectively to reflect the effectiveness of the proposed method. After running CPF, a loading margin of 4.03 was found in the system. It means that when the loading reaches 4.03 times system's base load, the voltage collapse occurs. Fig. 7 demonstrates the system's PV curves without SVC and with SVC at bus 9. For the SVC connected at bus 9, system loading margin increases from 4.03 to 4.17.

After running the CPF, bus voltage values found are shown in Fig. 8. The generally accepted technique is that optimal location for the SVC is the weakest bus (bus 5). Fig. 9 shows the comparison of bus voltage values in case SVC is installed

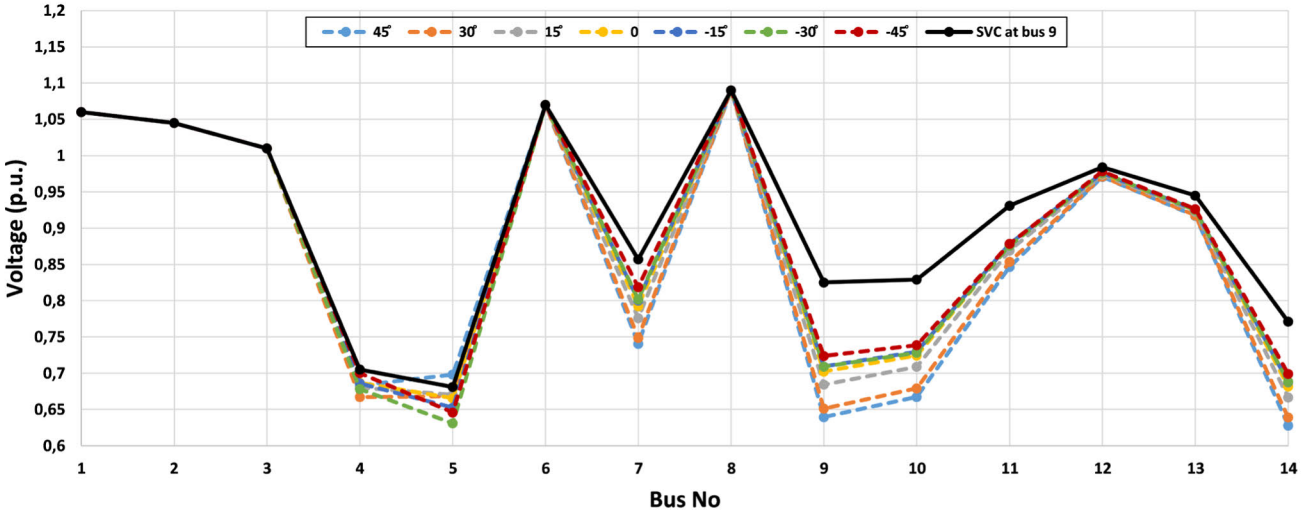

FIGURE 10. Comparison of PST with different angle values with SVC at bus 9.

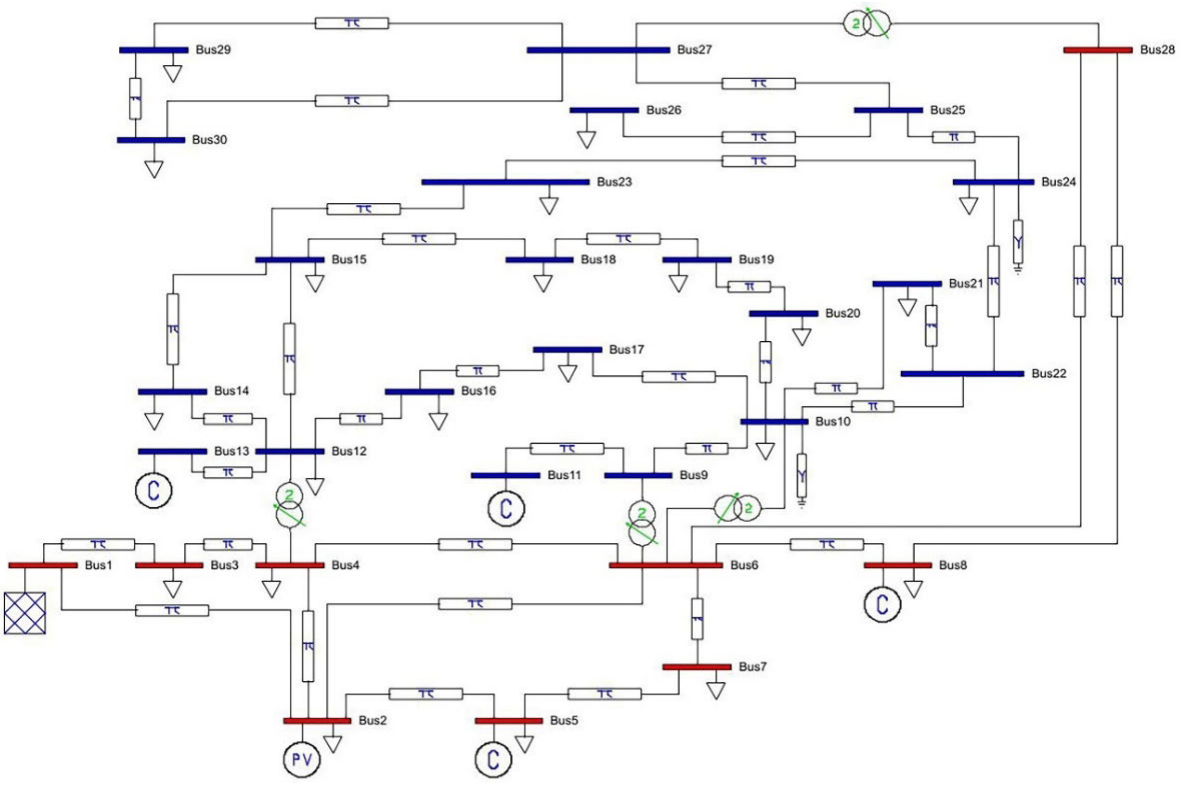

FIGURE 11. IEEE 30-bus system's PSAT model.

in bus 5 and bus 9. It is clearly seen that bus 5 is a worse location in terms of voltage profile.

Furthermore, the loadability limit, which indicates the power transmission capacity of the components in the network, increases from 2.88 to 3.37 for the SVC connected to Bus 9. Fig. 9 shows the voltage profile of the system where the loading factor is equal to 3.37. From Fig. 9, it can be seen that even when the system is overloaded, the SVC connected to bus 9 improves the voltage profile.

In power system operation, it is possible to determine the overloaded lines and transmission limits in the network under the operating conditions determined by the load flow analysis. In addition, the reliability of the system is also tested with the contingency analysis made to observe the

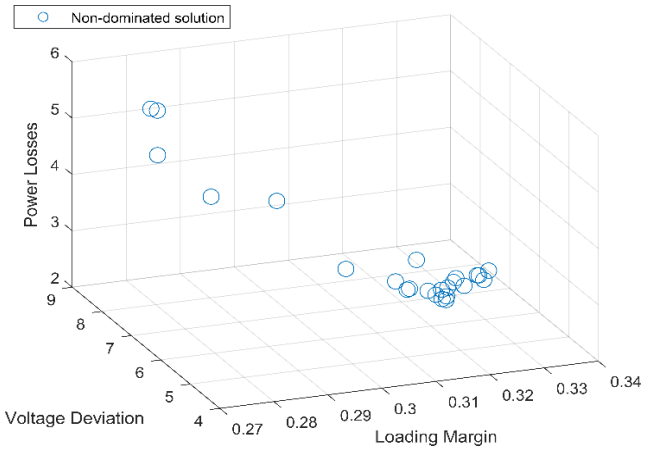

FIGURE 12. Optimal location of SVC for three objectives.

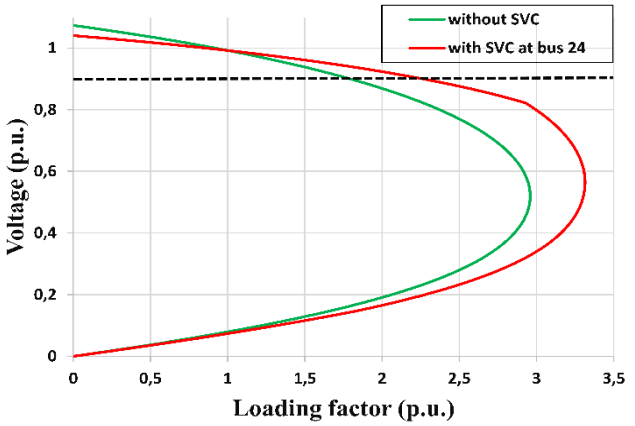

FIGURE 13. PV curves for IEEE 30-bus system without SVC and with SVC at bus 24.

TABLE 7. Minimum values of objective function in IEEE 30-bus test system.

Bus No.	f_1	f_2	f_3	F
3	0.04431	0.04440	0.03143	0.04326
4	0.04424	0.04490	0.03212	0.04336
6	0.04415	0.04443	0.03260	0.04324
7	0.04455	0.04554	0.03233	0.04372
9	0.04319	0.04085	0.03498	0.04206
10	0.04212	0.03670	0.03748	0.04069
12	0.04334	0.03977	0.03483	0.04195
14	0.04314	0.03976	0.03675	0.04196
15	0.04254	0.03743	0.03665	0.04107
16	0.04271	0.03765	0.03676	0.04124
17	0.04223	0.03584	0.03716	0.04058
18	0.04234	0.03434	0.03784	0.04042
19	0.04223	0.03347	0.03782	0.04018
20	0.04216	0.03375	0.03790	0.04018
21	0.04165	0.03657	0.03857	0.04041
22	0.04154	0.03601	0.03892	0.04026
23	0.04133	0.03681	0.04037	0.04038
24	0.04029	0.03844	0.04307	**0.04016**
25	0.03774	0.04584	0.05628	0.04084
26	0.03948	0.04704	0.05244	0.04202
27	0.03695	0.05091	0.06250	0.04176
28	0.04286	0.04648	0.03588	0.04298
29	0.03739	0.05667	0.06785	0.04364
30	0.03752	0.05641	0.06748	0.04365

Bold value shows the most suitable location where the objective function is minimum.

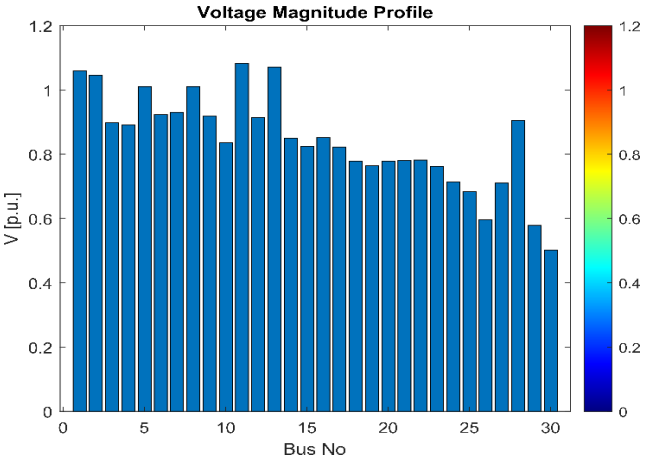

FIGURE 14. IEEE 30-bus system's voltage profile without SVC.

effect of a transmission line or generator outage in the system. Contingency analysis is the study of the effects on line power flows and bus voltages of the remaining system in case outage of any element (N-1 criterion). Thus, the measures to be taken in such a case are tried to be determined in advance [56]–[58].

In this study, contingency analysis was performed by outage of the transmission lines one by one in the IEEE 14-bus test system. The new objective function values and optimal SVC locations for each case are summarized in Table 5.

In the normal operating state, the values in the first three rows were close to each other and bus 9 was found to be the optimal placement. As can be seen from Table 5, the most suitable location in half of the contingency situations is the bus 14. Bus 9 for outage of five different lines and bus 10 for outage of two different lines is the optimal SVC location. Considering the contingencies, it would be more accurate to place the SVC on the bus 14. It is also noteworthy that the bus 4 and bus 11, which previously had high objective function values, were found to be the most suitable location for the three different line outage cases.

The Phase-Shifting Transformer (PST) is a special type of transformer used to control the power flow on the transmission line. Thanks to the special winding in its construction, the output voltage has a different phase angle from the input voltage. This can also be expressed as supplying a voltage with a different phase angle to the power system. The main function of PST is to control the power flowing on the transmission line by changing the phase angle [59], [60]. The phase angle in the PST must be chosen carefully as overloading the transformer will worsen the primary side voltage and destroy the equipment [61].

In this study, the effects of PST on the test system were examined and the results were compared with SVC. For this purpose, the most loaded transformer in the network (between bus 5 and bus 6) was changed with PST and phase angle range was determined between $-45°$ to $+45°$. Loading factor,

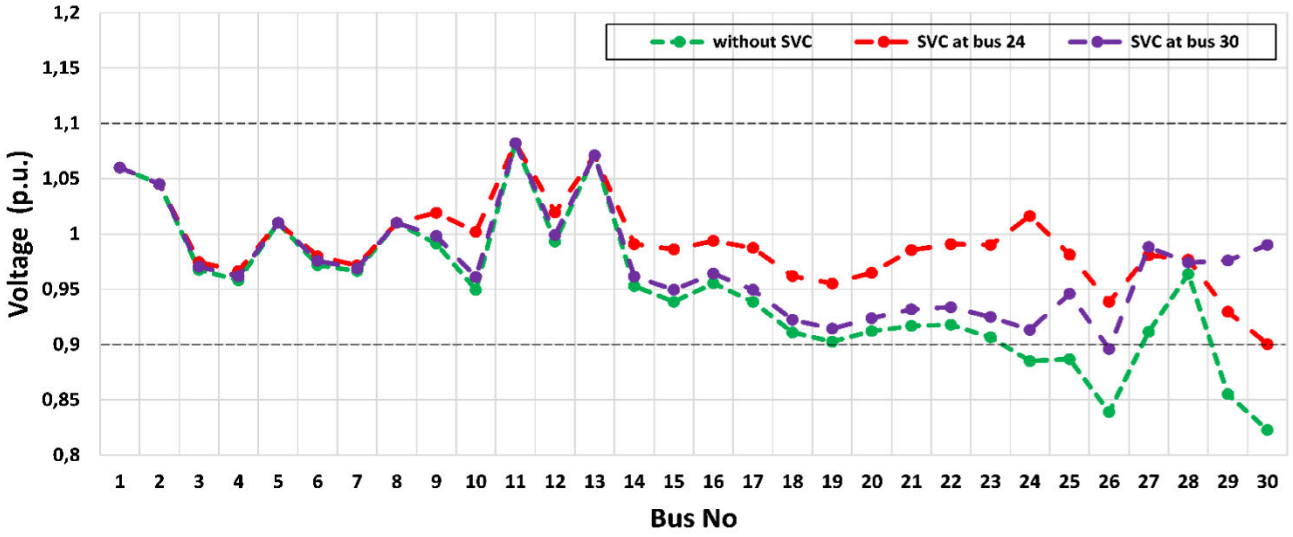

FIGURE 15. Voltage profile of test system without SVC, with SVC at bus 24 and with SVC at bus 30.

TABLE 8. Values of overloaded lines before and after placement of SVC.

Contingency	Overloaded lines	Overloading percentage of transmission line	Overloading percentage after SVC placement	SVC location
1-2	1-3	240.4	-	-
	3-4	211.2	-	-
	4-6	190.5	-	-
1-3	2-4	132.3	-	-
	2-6	142.6	-	-
	6-8	110.3	92.6	Bus 6
2-4	2-6	122.8	-	-
	6-8	106.2	92.5	Bus 6
2-5	2-4	115.1	-	-
	2-6	158.2	-	-
	4-6	135.3	-	-
2-6	2-4	109.6	-	-
	4-6	128.4	-	-
	6-8	109.8	91.9	Bus 6
3-4	2-4	130.5	-	-
	2-6	141.2	-	-
	6-8	110.3	92.6	Bus 6
4-6	2-6	151.7	-	-
	4-12	103.9	-	-
4-12	2-6	101.2	-	-
	4-6	123.9	-	-
	6-8	100.5	97.3	Bus 6
6-8	6-28	150.6	-	-
	8-28	103.4	95.9	Bus 28
6-9	6-8	101.3	95.0	Bus 6
6-28	6-8	144.3	-	-
9-11	6-8	102.2	92.5	Bus 6
10-20	15-18	102.0	95.2	Bus 18
27-28	22-24	127.0	-	-
	24-25	121.7	-	-

power losses and bus voltage values obtained according to different angles are given in Table 6.

As it is clearly seen in the table, when the PST angle value is changed, the loadability of the system decreased, and the power losses first increased and then started to decrease. Compared to the case of SVC at bus 9, it is seen that the power losses are lower at all phase angle values. However, SVC gave better results in load factor and busbar voltage values. In the base load voltage profile of the system given in Fig. 10, the application results of SVC and PST were compared. Considering the criterion weights, it would be more accurate to install SVC in the system in terms of voltage stability. PST can be used in applications that aim to reduce power losses.

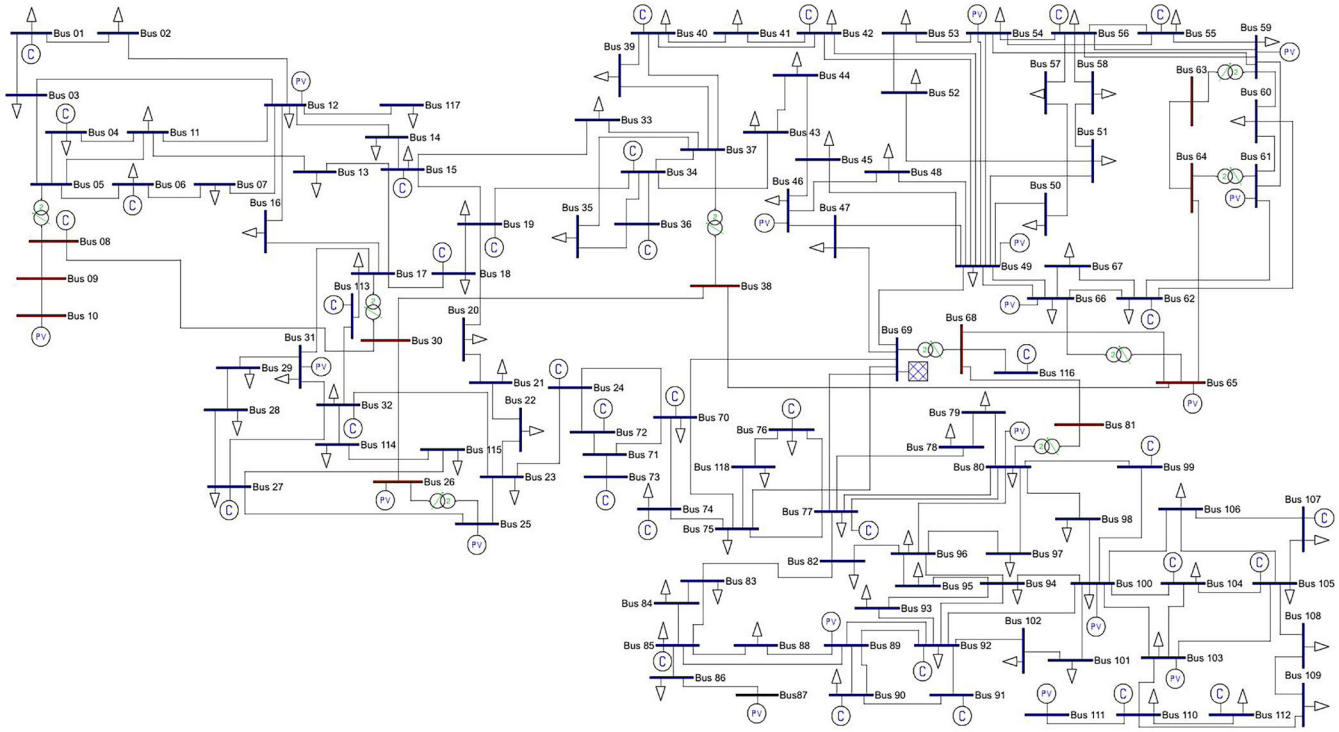

FIGURE 16. IEEE 118-bus system's PSAT model.

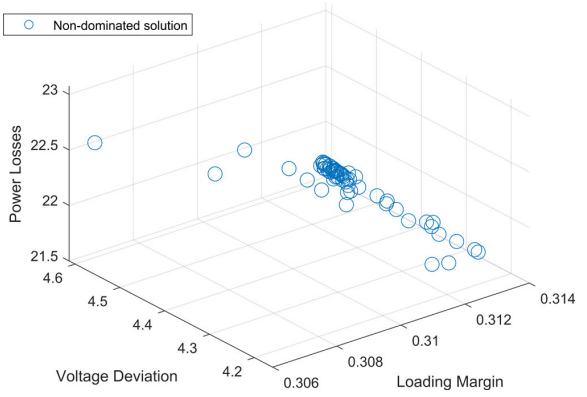

FIGURE 17. Optimal location of SVC for three objectives.

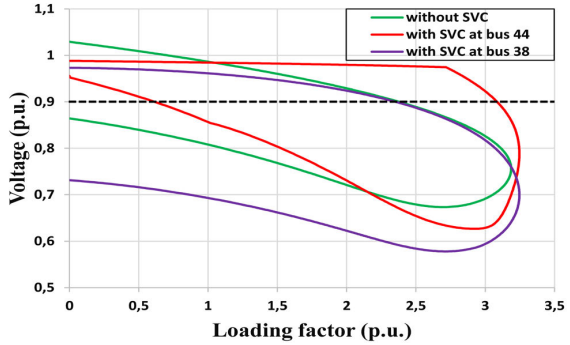

FIGURE 18. PV curves for IEEE 118-bus system.

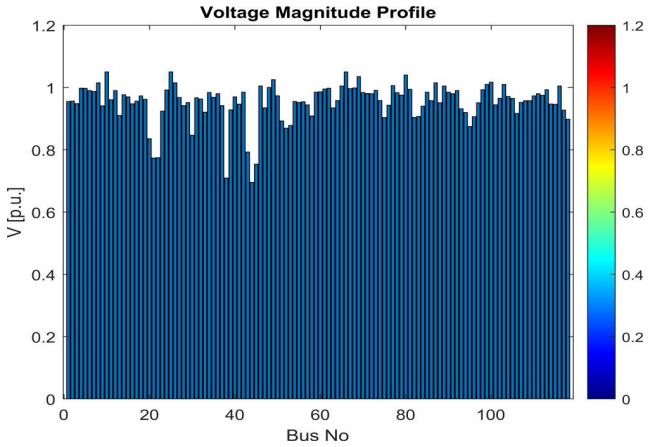

FIGURE 19. IEEE 118-bus system's voltage profile without SVC.

- IEEE 30-bus

The proposed method has also been tested on the IEEE 30 bus system. Fig. 11 shows the IEEE 30-bus network. There are six synchronous machines in this system, generators at bus 1 and 2, and synchronous capacitors for reactive power support at bus 5, 8, 11 and 13. Test system consists of 41 transmission lines and 30 buses with 21 loads. Total active and reactive loads in the system are 283.4 MW and 126.2 MVAr respectively.

Since the reactive power limits of the generator are taken into account, the objective function F is calculated at a loading factor near to the critical point. Fig. 12 demonstrates SVC's optimal location for three objectives.

Criteria values in the decision matrix were converted to proportional values in order not to dominate to each other. Table 7 shows the calculation results of the proposed

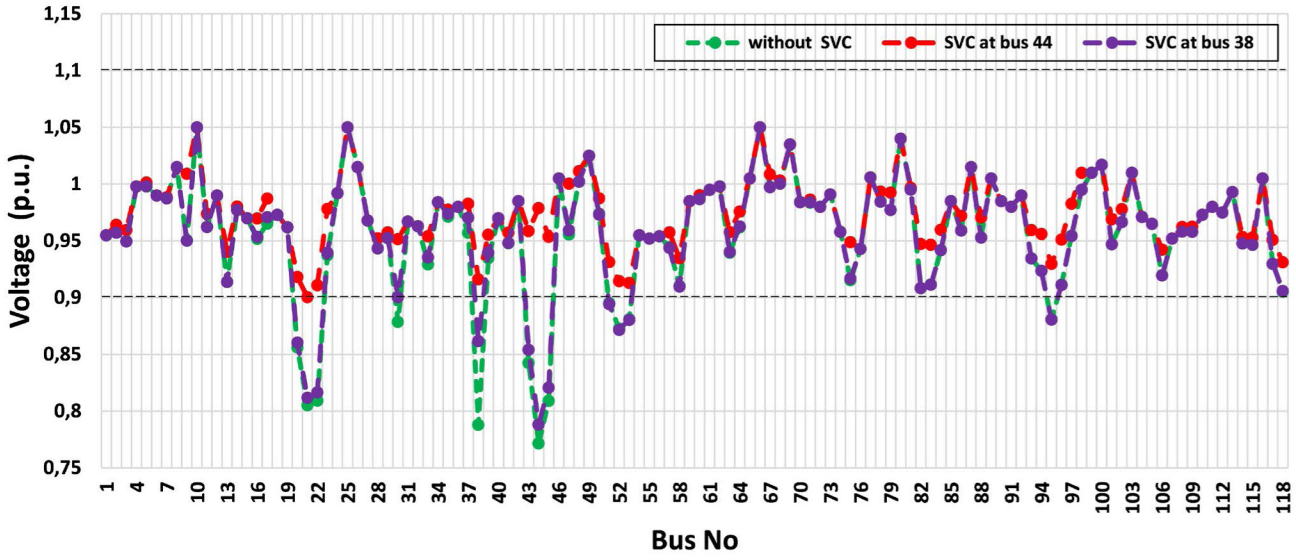

FIGURE 20. Voltage profile of test system without SVC, with SVC at bus 44 and with SVC at bus 38.

approach and also emphasizes that the best place for SVC is bus 24 in this test system.

Table 7 obviously demonstrates the importance of the MCDM technique used in this study in combining identified objectives and sustaining the minimum level of satisfaction for the objective function. It can be observed from Table 7 that bus 3 provides minimum power losses but, loading margin is not acceptable. Similarly, bus 19 gives the best value in voltage deviation and desirable value in active power loss but, loading margin is very high. The comparison outcomes for loading factor and voltage profile without SVC and with SVC connected at bus 24 are shown in Figs. 13, 14 and 15 respectively to reflect the effectiveness of the proposed method. After running CPF, a loading margin of 2.96 was found in the system. It means that when the loading reaches 2.96 times system's base load, the voltage collapse occurs. Fig. 13 demonstrates the system's PV curves without SVC and with SVC at bus 24. For the SVC connected at bus 24, system loading margin increases from 2.96 to 3.31.

After running the CPF, bus voltage values found are shown in Fig. 14. The generally accepted technique is that optimal location for the SVC is the weakest bus (bus 30). Fig. 15 shows the comparison of bus voltage values in case SVC is installed in bus 24 and bus 30. It is clearly seen that bus 30 is a worse location in terms of voltage profile.

Furthermore, the loadability limit, which indicates the power transmission capacity of the components in the network, increases from 1.79 to 2.26 for the SVC connected to bus 14. Fig. 15 shows the system's voltage profile at a loading factor of $\lambda = 2.26$. From Fig. 15, it can be seen that even when the system is overloaded, the SVC connected to bus 24 improves the voltage profile.

There are various factors that can cause contingency in power systems such as generator outage, line outage and overloads and these cause extreme situations such as voltage collapse, overloads in other branches, sudden system voltage rise or drop [62]. Contingencies occur in the power systems when the MVA rating of the transmission line exceeds certain limit values and several types of corrective actions are required to solve such problems [63]. IEEE 14-bus and 30 bus test systems don't have line limits. Line and transformer limits have been proposed by the authors in several articles [64]–[66]. In this study, the line limits suggested in [65] were used and congestion was created in the lines for the simulation purposes. To this end, line overloads were created by considering line outages. The percentage values of the overloaded lines before and after SVC placement are given in Table 8.

In the IEEE 30-bus system, there are no overloaded lines in 27 cases for 41 contingency scenarios. Although there are 33 overloaded lines in the other 14 cases, the power flowing to only 11 lines has decreased below the limit values with the installation of SVC on the proper buses. However, it is noteworthy that the SVC placed at the bus 6 solves the overloading problem in the line between the bus 6 and bus 8 in almost all cases. As seen at Table 8, in the case of contingency, SVC at the buses does not improve the condition of the overloaded lines. As a matter of fact, shunt compensators absorb or inject current from the line like a current source, so they are mostly used to control the voltage around the connection point. In accordance with this purpose, FACTS devices such as UPFC and TCSC (Thyristor Controlled Series Compensator) can be used to control the power flow in the network and solve the overloading problem in the lines.

- IEEE 118-bus

In order to demonstrate the effectiveness of the proposed method, it is finally tested on the IEEE 118-bus system. Fig. 16 shows the IEEE 118-bus network. There are nineteen generators and thirty-five synchronous capacitors in this system. Test system consists of 177 transmission lines and 118 buses with 91 loads. Total active and reactive loads in the system are 3668 MW and 1438 MVAr respectively.

TABLE 9. Minimum values of objective function in IEEE 14-bus test system.

Bus No.	f_1	f_2	f_3	F
Bus 02	0.01565	0.01591	0.01557	0.01570
Bus 03	0.01565	0.01590	0.01556	0.01569
Bus 05	0.01565	0.01596	0.01557	0.01571
Bus 07	0.01565	0.01597	0.01558	0.01571
Bus 09	0.01560	0.01582	0.01561	0.01564
Bus 11	0.01565	0.01584	0.01555	0.01567
Bus 13	0.01564	0.01571	0.01560	0.01565
Bus 14	0.01565	0.01594	0.01558	0.01570
Bus 16	0.01565	0.01582	0.01557	0.01567
Bus 17	0.01559	0.01591	0.01566	0.01566
Bus 20	0.01560	0.01501	0.01570	0.01549
Bus 21	0.01555	0.01447	0.01573	0.01536
Bus 22	0.01553	0.01448	0.01575	0.01534
Bus 23	0.01557	0.01556	0.01570	0.01558
Bus 28	0.01565	0.01587	0.01557	0.01569
Bus 29	0.01565	0.01591	0.01557	0.01570
Bus 30	0.01546	0.01581	0.01585	0.01556
Bus 33	0.01565	0.01590	0.01556	0.01569
Bus 35	0.01565	0.01593	0.01556	0.01570
Bus 37	0.01554	0.01598	0.01582	0.01564
Bus 38	0.01531	0.01599	0.01617	0.01551
Bus 39	0.01564	0.01585	0.01562	0.01568
Bus 41	0.01565	0.01588	0.01556	0.01569
Bus 43	0.01553	0.01515	0.01604	0.01550
Bus 44	0.01537	0.01442	0.01659	**0.01529**
Bus 45	0.01540	0.01450	0.01630	0.01530
Bus 47	0.01565	0.01573	0.01551	0.01566
Bus 48	0.01565	0.01588	0.01556	0.01569
Bus 50	0.01566	0.01580	0.01556	0.01568
Bus 51	0.01566	0.01513	0.01553	0.01554
Bus 52	0.01566	0.01512	0.01557	0.01554
Bus 53	0.01565	0.01540	0.01552	0.01559
Bus 57	0.01566	0.01582	0.01557	0.01568
Bus 58	0.01566	0.01548	0.01553	0.01561
Bus 60	0.01565	0.01595	0.01557	0.01571
Bus 63	0.01565	0.01585	0.01557	0.01568
Bus 64	0.01565	0.01589	0.01558	0.01569
Bus 67	0.01565	0.01587	0.01557	0.01569
Bus 68	0.01566	0.01596	0.01557	0.01571
Bus 71	0.01565	0.01596	0.01558	0.01571
Bus 75	0.01564	0.01573	0.01550	0.01565
Bus 78	0.01565	0.01586	0.01554	0.01568
Bus 79	0.01565	0.01579	0.01553	0.01567
Bus 81	0.01565	0.01597	0.01558	0.01571
Bus 82	0.01565	0.01493	0.01552	0.01550
Bus 83	0.01565	0.01517	0.01554	0.01555
Bus 84	0.01565	0.01571	0.01560	0.01566
Bus 86	0.01565	0.01584	0.01557	0.01568
Bus 88	0.01565	0.01581	0.01553	0.01568
Bus 93	0.01565	0.01555	0.01555	0.01563
Bus 94	0.01565	0.01507	0.01551	0.01553
Bus 95	0.01565	0.01479	0.01553	0.01548
Bus 96	0.01565	0.01477	0.01553	0.01547
Bus 97	0.01565	0.01547	0.01555	0.01561
Bus 98	0.01565	0.01584	0.01557	0.01568
Bus 101	0.01565	0.01569	0.01554	0.01565
Bus 102	0.01565	0.01582	0.01556	0.01568
Bus 106	0.01565	0.01583	0.01557	0.01568
Bus 108	0.01565	0.01592	0.01558	0.01570
Bus 109	0.01565	0.01591	0.01558	0.01570
Bus 114	0.01565	0.01587	0.01557	0.01569
Bus 115	0.01565	0.01586	0.01557	0.01569
Bus 117	0.01565	0.01576	0.01557	0.01567
Bus 118	0.01565	0.01575	0.01554	0.01566

Bold value shows the most suitable location where the objective function is minimum.

In IEEE 14-bus and 30 bus test systems, the rated values of SVC were taken between −100 MVAr and +100 MVAr. IEEE 118-bus test system is a larger network model; therefore, the SVC is rated as −300/+300 MVAr in order to see the effect of compensation more clearly. Since the reactive power limits of the generator are taken into account, the objective function F is calculated at a loading factor near to the critical point. Fig. 17 demonstrates SVC's optimal location for three objectives.

Criteria values in the decision matrix were converted to proportional values in order not to dominate to each other. Table 9 shows the calculation results of the proposed approach and also emphasizes that the best place for SVC is bus 44 in this test system.

Table 9 obviously demonstrates the importance of the MCDM technique used in this study in combining identified objectives and sustaining the minimum level of satisfaction for the objective function. It can be observed from Table 9 that bus 44 gives the best value in voltage deviation and second best in loading margin, but in the worst location in terms of active power losses. Similarly, bus 38 has the best value in loading margin, and interestingly, it has the worst value in voltage deviation. After running CPF, a loading margin of 3.19 was found in the system. It means that when the loading reaches 3.19 times system's base load, the voltage collapse occurs. Fig. 18 demonstrates the system's PV curves without SVC and with SVC at bus 38 and bus 44. For the SVC connected at bus 44, system loading margin increases from 3.19 to 3.21.

After running the CPF, bus voltage values found are shown in Fig. 19. It is noteworthy that, unlike other IEEE test systems, the optimal location for SVC is the weakest bus (bus 44). Fig. 20 shows the comparison of bus voltage values in case SVC is installed in bus 44 and bus 38.

Furthermore, the loadability limit, which indicates the power transmission capacity of the components in the network, increases from 2.38 to 3.08 for the SVC connected to bus 44. Fig. 20 shows the voltage profile of the system where the loading factor is equal to 3.08. From Fig. 20, it can be seen that even when the system is overloaded, the SVC connected to bus 44 improves the voltage profile. It is clearly seen that bus 38 with the best loading margin gives similar results in terms of voltage profile as the case without SVC.

VI. CONCLUSION

A MCDM method was proposed in this paper using AHP technique to improve voltage stability. On the IEEE 14-bus, IEEE 30-bus and IEEE 118-bus test systems, this method's efficiency has been indicated. The method attempted to optimize allocation of the FACTS controller according to three goals: increasing the loading margin, reducing voltage deviation and reducing active power losses. By using objective function ranking, optimal SVC location has presented among the weakest buses. It has been identified that SVC can be placed optimally in bus 9 for the IEEE 14-bus system, bus 24 for the IEEE 30-bus system and bus 44 for the IEEE 118-bus system. By applying this approach to actual systems, power system operators can be provided with useful information for voltage stability and its improvement. The results presented by this approach are promising and promoting for possible applications. This method can be also useful in larger power systems for various FACTS placement strategies. Different contingencies were analyzed in the IEEE 14-bus test system and bus 14 was found to be the most appropriate location in half of the line outages. It has also been shown that

SVC on buses does not improve the condition of overloaded lines in case of contingencies. In addition, the effects of PST on the test system were examined and the results were compared with SVC. It has been seen that SVC gives better results in loading margin and bus voltage values.

The present research focused on only three objectives. Future studies might include other objectives such as cost minimization in generator units, FACTS installation cost reduction, etc. Additionally, different FACTS devices such as STATCOM may be used or the number of controllers may be increased in future applications.

REFERENCES

[1] G. N. Kumar and M. S. Kalavathi, "Cat swarm optimization for optimal placement of multiple UPFC's in voltage stability enhancement under contingency," *Electr. Power Energy Syst.*, vol. 57, pp. 97–104, May 2014, doi: 10.1016/j.ijepes.2013.11.050.

[2] A. Gupta and P. R. Sharma, "Static and transient voltage stability assessment of power system by proper placement of UPFC with POD controller," *WSEAS Trans. Power Syst.*, vol. 8, no. 4, pp. 197–206, Oct. 2013.

[3] R. Sirjani, A. Mohamed, and H. Shareef, "Optimal allocation of shunt VAR compensators in power systems using a novel global harmony search algorithm," *Int. J. Electr. Power Energy Syst.*, vol. 43, no. 1, pp. 562–572, Dec. 2012, doi: 10.1016/j.ijepes.2012.05.068.

[4] R. Kalaivani and V. Kamaraj, "Enhancement of voltage stability by optimal location of static VAR compensator using genetic algorithm and particle swarm optimization," *Amer. J. Eng. Appl. Sci.*, vol. 5, no. 1, pp. 70–77, May 2012, doi: 10.3844/ajeassp.2012.70.77.

[5] S. Galvani, B. Mohammadi-Ivatloo, M. Nazari-Heris, and S. Rezaeian-Marjani, "Optimal allocation of static synchronous series compensator (SSSC) in wind-integrated power system considering predictability," *Electr. Power Syst. Res.*, vol. 191, pp. 1–13, Feb. 2021, doi: 10.1016/j.epsr.2020.106871.

[6] A. Amarendra, L. R. Srinivas, and R. S. Rao, "Identification of the best location and size of IPFC to optimize the cost and to improve the power system security using firefly optimization algorithm," *Mater. Today, Proc.*, Dec. 2020, doi: 10.1016/j.matpr.2020.11.318.

[7] M. El-Azab, W. A. Omran, S. F. Mekhamer, and H. E. A. Talaat, "Allocation of FACTS devices using a probabilistic multi-objective approach incorporating various sources of uncertainty and dynamic line rating," *IEEE Access*, vol. 8, pp. 167647–167664, 2020, doi: 10.1109/ACCESS.2020.3023744.

[8] A. Gautam, P. Sahrma, and Y. Kumar, "Congestion management by sensitivity based approach for optimal allocation & parameter setting of TCSC using grey wolf optimisation," in *Proc. ICPC2T*, Raipur, India, Jan. 2020, pp. 50–55, doi: 10.1109/ICPC2T48082.2020.9071487.

[9] O. A. Coronado de Koster, J. S. Artal-Sevil, and J. A. Dominguez-Navarro, "Multi-type FACTS location in a microgrid," in *Proc. EVER*, Monte Carlo, Monaco, Sep. 2020, pp. 1–5, doi: 10.1109/EVER48776.2020.9243070.

[10] S. Rezaeian-Marjani, S. Galvani, V. Talavat, and M. Farhadi-Kangarlu, "Optimal allocation of D-STATCOM in distribution networks including correlated renewable energy sources," *Int. J. Electr. Power Energy Syst.*, vol. 122, pp. 1–14, Nov. 2020, doi: 10.1016/j.ijepes.2020.106178.

[11] A. A. Shehata, A. Refaat, and N. V. Korovkin, "Optimal allocation of FACTS devices based on multi-objective multi-verse optimizer algorithm for multi-objective power system optimization problems," in *Proc. FarEastCon*, Vladivostok, Russia, Oct. 2020, doi: 10.1109/FarEastCon50210.2020.9271359.

[12] X. Shen, H. Luo, W. Gao, Y. Feng, and N. Feng, "Evaluation of optimal UPFC allocation for improving transmission capacity," *Global Energy Interconnection*, vol. 3, no. 3, pp. 217–226, Jun. 2020, doi: 10.1016/j.gloei.2020.07.003.

[13] S. Thiruvenkadam, H.-J. Kim, and I.-H. Ra, "Optimal sizing and location identification of suitable compensator in a radial distribution network through fuzzy-flower pollination optimization algorithm," in *Proc. ICICT*, Coimbatore, India, Feb. 2020, pp. 576–583, doi: 10.1109/ICICT48043.2020.9112450.

[14] B. V. Kumar and V. Ramaiah, "Enhancement of dynamic stability by optimal location and capacity of UPFC: A hybrid approach," *Energy*, vol. 190, Jan. 2020, Art. no. 116464, doi: 10.1016/j.energy.2019.116464.

[15] A. K. Arya, A. Kumar, and S. Chanana, "Analysis of distribution system with D-STATCOM by gravitational search algorithm (GSA)," *J. Inst. Eng. India B*, vol. 100, no. 3, pp. 207–215, Feb. 2019, doi: 10.1007/s40031-019-00383-2.

[16] K. Balamurugan and K. Muthukumar, "Differential evolution algorithm for contingency analysis-based optimal location of FACTS controllers in deregulated electricity market," *Soft Comput.*, vol. 23, no. 1, pp. 163–179, Jan. 2019, doi: 10.1007/s00500-018-3141-x.

[17] E. A. Belati, C. F. Nascimento, H. de Faria, E. H. Watanabe, and A. Padilha-Feltrin, "Allocation of static VAR compensator in electric power systems considering different load levels," *J. Control, Autom. Electr. Syst.*, vol. 30, no. 1, pp. 1–8, Oct. 2018, doi: 10.1007/s40313-018-00421-2.

[18] S. Dawn, P. K. Tiwari, and A. K. Goswami, "An approach for long term economic operations of competitive power market by optimal combined scheduling of wind turbines and FACTS controllers," *Energy*, vol. 181, pp. 709–723, Aug. 2019, doi: 10.1016/j.energy.2019.05.225.

[19] S. Galvani, M. T. Hagh, M. B. B. Sharifian, and B. Mohammadi-Ivatloo, "Multiobjective predictability-based optimal placement and parameters setting of UPFC in wind power included power systems," *IEEE Trans. Ind. Informat.*, vol. 15, no. 2, pp. 878–888, Feb. 2019, doi: 10.1109/TII.2018.2818821.

[20] M. Rambabu, G. V. N. Kumar, and S. Sivanagaraju, "An intermittent contingency approach with optimal placement of static VAR compensator in a renewable-integrated power systems," *Int. J. Ambient Energy*, vol. 42, no. 13, pp. 1551–1561, May 2019, doi: 10.1080/01430750.2019.1611649.

[21] V. V. S. N. Murty and A. Kumar, "Impact of D-STATCOM in distribution systems with load growth on stability margin enhancement and energy savings using PSO and GAMS," *Int. Trans. Electr. Energy Syst.*, vol. 28, no. 11, pp. 1–24, Jun. 2018, doi: 10.1002/etep.2624.

[22] Y. Amrane and N. E. L. Y. Kouba, "A multiobjective optimal VAR dispatch using FACTS devices considering voltage stability and contingency analysis," in *Predictive Modelling for Energy Management and Power Systems Engineering*, 1st ed. Amsterdam, The Netherlands: Elsevier, 2020, ch. 1, pp. 1–26, doi: 10.1016/B978-0-12-817772-3.00001-X.

[23] S. S. Padaiyatchi, "Hybrid DE/FFA algorithm applied for different optimal reactive power dispatch problems," *Austral. J. Electr. Electron. Eng.*, vol. 17, no. 3, pp. 203–210, Sep. 2020, doi: 10.1080/1448837X.2020.1817233.

[24] M. Nadeem, M. Z. Zeb, K. Imran, and A. K. Janjua, "Optimal sizing and allocation of SVC and TCSC in transmission network by combined sensitivity index and PSO," in *Proc. ICAEM*, Taxila, Pakistan, Aug. 2019, pp. 111–116, doi: 10.1109/ICAEM.2019.8853759.

[25] B. Singh, V. Mukherjee, and P. Tiwari, "GA-based optimization for optimally placed and properly coordinated control of distributed generations and static VAR compensator in distribution networks," *Energy Rep.*, vol. 5, pp. 926–959, Nov. 2019, doi: 10.1016/j.egyr.2019.07.007.

[26] R. Sirjani, "Optimal placement and sizing of PV-STATCOM in power systems using empirical data and adaptive particle swarm optimization," *Sustainability*, vol. 10, no. 3, p. 727, Mar. 2018, doi: 10.3390/su10030727.

[27] A. R. Jordehi, "Brainstorm optimisation algorithm (BSOA): An efficient algorithm for finding optimal location and setting of FACTS devices in electric power systems," *Int. J. Elect. Power Energy Syst.*, vol. 69, pp. 48–57, Jul. 2015, doi: 10.1016/j.ijepes.2014.12.083.

[28] K. Ravi and M. Rajaram, "Optimal location of FACTS devices using improved particle swarm optimization," *Int. J. Electr. Power Energy Syst.*, vol. 49, pp. 333–338, Jul. 2013, doi: 10.1016/j.ijepes.2012.12.008.

[29] M. Davoodi, M. Davoudi, I. Ganjkhany, and A. Aref, "Optimal capacitor placement in distribution networks using genetic algorithm," *Indian J. Sci. Technol.*, vol. 5, no. 7, pp. 3054–3058, Jul. 2012, doi: 10.17485/ijst/2012/v5i7.15.

[30] M. J. Sanjari, H. Fathi, G. B. Gharehpetian, and A. Tavakoli, "HSA-based optimal placement of shunt FACTS devices in the smart grid considering voltage stability," in *Proc. ICSG*, Tehran, Iran, 2012, pp. 1–6.

[31] A. A. Sadiq, S. S. Adamu, and M. Buhari, "Optimal distributed generation planning in distribution networks: A comparison of transmission network models with FACTS," *Eng. Sci. Technol., Int. J.*, vol. 22, no. 1, pp. 33–46, Feb. 2019, doi: 10.1016/j.jestch.2018.09.013.

[32] S. S. S. Kapse, M. B. Daigavane, and P. M. Daigavane, "Optimal localization and sizing of UPFC to solve the reactive power dispatch problem under unbalanced conditions," *IETE J. Res.*, vol. 66, no. 3, pp. 396–413, May 2020, doi: 10.1080/03772063.2018.1491808.

[33] S. K. Mahmoudi, M. E. H. Golshan, and R. Zamani, "Coordinated voltage control scheme for transmission system considering objectives and constraints of network and control devices," *Electr. Power Syst. Res.*, vol. 192, Mar. 2021, Art. no. 106908, doi: 10.1016/j.epsr.2020.106908.

[34] S. R. Marjani, V. Talavat, and S. Galvani, "Optimal allocation of D-STATCOM and reconfiguration in radial distribution network using MOPSO algorithm in TOPSIS framework," *Int. Trans. Electr. Energy Syst.*, vol. 29, no. 2, p. e2723, Feb. 2019, doi: 10.1002/etep.2723.
[35] M. B. Shafik, H. Chen, G. I. Rashed, and R. A. El-Sehiemy, "Adaptive multi objective parallel seeker optimization algorithm for incorporating TCSC devices into optimal power flow framework," *IEEE Access*, vol. 7, pp. 36934–36947, 2019, doi: 10.1109/ACCESS.2019.2905266.
[36] M. B. Shafik, G. I. Rashed, R. A. El-Sehiemy, and H. Chen, "Optimal sizing and sitting of TCSC devices for multi-objective operation of power systems using adaptive seeker optimization algorithm," in *Proc. Tensymp*, Sydney, NSW, Australia, Jul. 2018, pp. 231–236.
[37] N. Hingorani and L. Gyugyi, *Understanding FACTS: Concepts and Technology Flexible AC Transmission Systems*, vol. 1. New York, NY, USA: IEEE Press, 2000, pp. 1–35.
[38] H. R. Muhammed, *Power Electronics, Devices, Circuits and Applications*. 4th ed. Essex, U.K.: Pearson, 2014, pp. 626–657.
[39] F. Nepsha, V. Voronin, R. Belyaevsky, V. Efremenko, and K. Varnavskiy, "Application of FACTS devices in power supply systems of coal mines," in *Proc. E3S Web Conf.*, 2020, p. 8, doi: 10.1051/e3sconf/202017403026.
[40] H. Samet, S. Ketabipour, M. Afrasiabi, S. Afrasiabi, and M. Mohammadi, "Deep learning forecaster based controller for SVC: Wind farm flicker mitigation," *IEEE Trans. Ind. Informat.*, early access, Sep. 18, 2020, doi: 10.1109/TII.2020.3025101.
[41] N. A. Skaria, S. Baby, and D. M. Anumodu, "Genetic algorithm based optimal location of SVC in power system for voltage stability enhancement," in *Proc. AICERA/iCMMD*, Kottayam, India, Jul. 2014, pp. 1–6.
[42] S. Shojaeian, E. S. Naeeni, M. Dolatshahi, and H. Khani, "A PSO-DP based method to determination of the optimal number, location, and size of FACTS devices in power systems," *Adv. Electr. Comput. Eng.*, vol. 14, no. 1, pp. 109–114, 2014, doi: 10.4316/AECE.2014.01017.
[43] H. H. Goh, B. C. Kok, H. T. Yeo, S. W. Lee, and A. A. M. Zin, "Combination of TOPSIS and AHP in load shedding scheme for large pulp mill electrical system," *Int. J. Electr. Power Energy Syst.*, vol. 47, pp. 198–204, May 2013, doi: 10.1016/j.ijepes.2012.10.059.
[44] S. Liu, Q. Zhao, M. Wen, L. Deng, S. Dong, and C. Wang, "Assessing the impact of hydroelectric project construction on the ecological integrity of the Nuozhadu nature reserve, southwest China," *Stochastic Environ. Res. Risk Assessment*, vol. 27, no. 7, pp. 1709–1718, Mar. 2013, doi: 10.1007/s00477-013-0708-z.
[45] A. Awasthi and S. S. Chauhan, "Using AHP and Dempster–Shafer theory for evaluating sustainable transport solutions," *Environ. Model. Softw.*, vol. 26, no. 6, pp. 787–796, Jun. 2011, doi: 10.1016/j.envsoft.2010.11.010.
[46] A. Mazza, G. Chicco, and A. Russo, "Optimal multi-objective distribution system reconfiguration with multi criteria decision making-based solution ranking and enhanced genetic operators," *Int. J. Electr. Power Energy Syst.*, vol. 54, pp. 255–267, Jan. 2014, doi: 10.1016/j.ijepes.2013.07.006.
[47] T. L. Saaty, "A scaling method for priorities in hierarchical structures," *J. Math. Psychol.*, vol. 15, no. 3, pp. 234–281, Jun. 1977, doi: 10.1016/0022-2496(77)90033-5.
[48] B. Cavallo and L. D'Apuzzo, "A general unified framework for pairwise comparison matrices in multicriterial methods," *Int. J. Intell. Syst.*, vol. 24, no. 4, pp. 377–398, Apr. 2009, doi: 10.1002/int.20329.
[49] V. Ajjarapu and C. Christy, "The continuation power flow: A tool for steady state voltage stability analysis," *IEEE Trans. Power Syst.*, vol. 7, no. 1, pp. 416–423, Feb. 1992, doi: 10.1109/59.141737.
[50] M. M. Aman, G. B. Jasmon, A. H. A. Bakar, and H. Mokhlis, "Optimum network reconfiguration based on maximization of system loadability using continuation power flow theorem," *Int. J. Electr. Power Energy Syst.*, vol. 54, pp. 123–133, Jan. 2014, doi: 10.1016/j.ijepes.2013.06.026.
[51] A. S. Telang and P. P. Bedekar, "Systematic approach for optimal placement and sizing of STATCOM to assess the voltage stability," in *Proc. ICCPCT*, Nagercoil, India, Mar. 2016, pp. 1–6.
[52] R. Benabid and M. Boudour, "Optimal location and size of SVC and TCSC for multi-objetive static voltage stability enhancement," *Renew. Energy Power Qual. J.*, vol. 1, no. 6, pp. 175–180, Mar. 2008.
[53] A. Laifa and A. Medoued, "Optimal FACTS location to enhance voltage stability using multi-objective harmony search," in *Proc. EPECS*, Istanbul, Turkey, Oct. 2013, pp. 1–6.
[54] A. R. Phadke, M. Fozdar, and K. R. Niazi, "A new multi-objective fuzzy-GA formulation for optimal placement and sizing of shunt FACTS controller," *Int. J. Electr. Power Energy Syst.*, vol. 40, no. 1, pp. 46–53, Sep. 2012, doi: 10.1016/j.ijepes.2012.02.004.
[55] F. Milano, "An open source power system analysis toolbox," *IEEE Trans. Power Syst.*, vol. 20, no. 3, pp. 1199–1206, Aug. 2005, doi: 10.1109/TPWRS.2005.851911.
[56] P. S. Vaidya and V. K. Chandrakar, "Contingency analysis of power network with STATCOM and SVC," in *Proc. ICEEE*, Singapore, 2021, pp. 121–130, doi: 10.1007/978-981-16-0749-3_9.
[57] P. Choudekar, S. K. Sinha, and A. Siddiqui, "Optimal location of SVC for improvement in voltage stability of a power system under normal and contingency condition," *Int. J. Syst. Assurance Eng. Manage.*, vol. 8, no. S2, pp. 1312–1318, Mar. 2017, doi: 10.1007/s13198-017-0601-0.
[58] G. A. Salman, "Power system security improvement by optimal location of fact's devices," *Int. J. Eng. Res. Technol.*, vol. 4, no. 2, pp. 610–616, Feb. 2015.
[59] M. A. Bhaskar, C. Subramani, M. J. Kumar, and S. S. Dash, "Voltage profile improvement using FACTS devices: A comparison between SVC, TCSC and TCPST," in *Proc. ARTCom*, Kottayam, India, 2009, pp. 890–892, doi: 10.1109/ARTCom.2009.135.
[60] S. Egoigwe, T. O. Araoye, and F. U. Ilo, "Improving power flow control in AC transmission system using phase shifting transformer (PST)," *Comput. Eng. Intell. Syst.*, vol. 11, no. 4, pp. 21–29, Jun. 2020.
[61] K. Abderrezak, T. Mesbah, and A. Djellad, "TCPST (thyristor control phase shifting transformer) impact on power quality," in *Proc. CIER*, Sousse, Tunisie, 2013, pp. 1–5.
[62] D. Asija, P. Choudekar, K. M. Soni, and S. K. Sinha, "Power flow study and contingency status of WSCC 9 bus test system using MATLAB," in *Proc. RDCAPE*, Noida, India, Mar. 2015, pp. 338–342, doi: 10.1109/RDCAPE.2015.7281420.
[63] R. Retnamony and I. Raglend, "N-1 contingency analysis in a congested power system and enhance the voltage stability using FACTS devices," in *Proc. IJCTA*, Jan. 2016, vol. 9, no. 7, pp. 3147–3157.
[64] S. Souag and F. Benhamida, "Secured economic dispatch algorithm using GSDF matrix," *Leonardo J. Sci.*, vol. 13, pp. 1–14, Jan./Jun. 2014.
[65] S. Verma, S. Saha, and V. Mukherjee, "A novel symbiotic organisms search algorithm for congestion management in deregulated environment," *J. Exp. Theor. Artif. Intell.*, vol. 29, no. 1, pp. 59–79, Jan. 2017, doi: 10.1080/0952813X.2015.1116141.
[66] J. Jobanputra and C. Kotwal, "Power flow management analysis using compensating techniques for managing congestion within electrical energy network," *Social Netw. Appl. Sci.*, vol. 3, no. 2, Jan. 2021, pp. 1–11, doi: 10.1007/s42452-021-04253-9.
[67] S. Verma and V. Mukherjee, "Firefly algorithm for congestion management in deregulated environment," *Eng. Sci. Technol., Int. J.*, vol. 19, no. 3, pp. 1254–1265, Sep. 2016, doi: 10.1016/j.jestch.2016.02.001.

FARUK AYDIN (Student Member, IEEE) received the B.Sc. degree in electrical and electronics engineering from Sakarya University, Sakarya, Turkey, in 2009, and the M.Sc. degree in electrical engineering from Yıldız Technical University (YTU), Istanbul, Turkey, in 2014. From 2011 to 2017, he worked with Ministry of Science, Industry and Technology, Turkey. He is currently a Research Assistant with the Department of Electrical and Electronics Engineering, Marmara University, Istanbul. His research interests include FACTS, power system stability, smart grids, optimization, and power quality.

BILAL GUMUS received the B.Sc. degree in electrical engineering from Istanbul Technical University (ITU), Istanbul, Turkey, in 1992, and the M.Sc. and Ph.D. degrees in electrical and electronics engineering from Fırat University, Elazıg, Turkey, in 1997 and 2004, respectively. He is currently working as an Associate Professor and the Head of the Department of Electrical-Electronics Engineering, Dicle University, Diyarbakır, Turkey. His research interests include electric machinery, power electronics, smart grids, and micro grids.